Reconstruction of Heterogeneous Materials via Stochastic Optimization of Limited-Angle X-Ray Tomographic Projections

Hechao Li [1], Nikhilesh Chawla [2], and Yang Jiao [2,*]

1. Mechanical Engineering, Arizona State University, Tempe, AZ 85287-6206

2. Materials Science and Engineering, Arizona State University, Tempe, AZ 85287-6206

Submitted to:

Scripta Materialia

June 2014

*Corresponding author (Email: yang.jiao.2@asu.edu)

Abstract

X-ray tomography has provided a non-destructive means for microstructure characterization in 3D and 4D. A stochastic procedure to accurately reconstruct material microstructure from limited-angle x-ray tomographic projections is presented and its utility is demonstrated by reconstructing a variety of distinct heterogeneous materials and elucidating the information content of different projection data sets. A small number of projections (e.g., 20 - 40) are necessary for accurate reconstructions via the stochastic procedure, indicating its high efficiency in using limited structural information.

Key words: Stochastic reconstruction, material microstructure, limited-angle projections

The physical properties and performance of heterogeneous materials are determined by their complex microstructures and how such microstructures evolve under various conditions [1-2]. Traditionally, the study of material microstructure has been limited by two dimensional (2D) imaging techniques. This approach is often inaccurate or inadequate for solving many cutting-edge problems. It is also often laborious and time-consuming. Advances in experimental methods, analytical techniques, and computational approaches, have now enabled the development of three dimensional (3D) analyses [3]. The study of 3D microstructures under an external stimulus (e.g., stress, temperature, and environment) as a function of time (i.e., 4D materials science) is also particularly exciting. Examples include an understanding of time-dependent deformation structures, phase transformations, compositional evolution, magnetic domains, to name just a few.

X-ray tomography is an extremely attractive, non-destructive technique for characterizing microstructure in 3D and 4D [4-6]. The use of high brilliance and partially coherent synchrotron light allows one to image multi-component materials from the sub-micrometer to nanometer range. In x-ray tomography, 2D projections are usually obtained at small angular increments. Given a sufficiently large number of such 2D projections, tomographic reconstruction techniques such as the filtered-back-projection algorithm [7], algebraic reconstruction techniques [8], as well as trajectory-based direct iterative reconstruction method [9] can be employed to generate a grayscale image of the microstructure. Further segmentation and thresholding analysis are used to resolve details of individual material phases and produce accurate digital representations of the 3D microstructure. Such data sets can be used to quantify the microstructure, and/or can be used as an input for microstructure-based modeling. Thus, x-ray tomography is an excellent technique that eliminates destructive cross-sectioning, and allows for superior resolution and image quality with minimal sample preparation [10-16].

The large number of 2D projections required for traditional reconstruction algorithms strongly limits the application of this technique in 4D materials science. An extremely large volume of data is usually needed as the input for the reconstruction algorithms even for a single “snapshot” of the microstructure at a given time-step. Characterizing an entire microstructural evolution process, at multiple time steps, may lead to hundreds of TB of data. Efficiently storing, retrieving, and

maintaining such large data streams are a significant challenge to the materials community. Therefore, it is highly desirable to devise alternative reconstruction procedures that can render accurate virtual microstructures from only a handful of 2D projections. This will not only significantly reduce the volume of tomography data required to characterize a 4D process but also improve the temporal resolution since the time interval between successive snapshots can be much shorter due to the smaller number of projections acquired.

If the material of interest only contains a small number of distinct phases and the phase properties (i.e., the attenuation coefficients) are known a priori (the focus of this paper), the reconstruction problem amounts to distributing different phases in a predefined discrete regular grid (e.g., simple cubic lattice), which is the focus of *discrete tomography* [17, 18]. Discrete tomography is closely related to several other mathematical fields, including number theory [19, 20], discrete geometry [21, 22] and combinatorics [23, 24]. It typically deals with reconstructions from a small number of projections and several associated algorithms have been devised. For example, the discrete algebraic reconstruction technique (DART) [25, 26] employs iterative segmentation of grayscale reconstructions to improve the accuracy for interface regions. The generic iterative methods [27] generally update a reconstruction for each projection angle separately, and thus, the convergence and accuracy of the reconstruction depends on the angle selection schemes. In addition, a stochastic method [28, 29] has been devised to improve the quality of pre-reconstructed grain maps.

Here, we present a stochastic optimization procedure to generate efficient and accurate reconstructions of heterogeneous material microstructures from limited-angle absorption contrast x-ray projections (i.e., limited tomography data). Our procedure is unique from previous discrete tomography reconstruction methods in several aspects: (i) no segmentation is needed in any stages of the reconstruction (in contrast to DART); (ii) projections of all angles are simultaneously considered and angle selections do not affect the convergence of the reconstruction (in contrast to the generic iterative methods); (iii) reconstructions both from scratch (random initial microstructure) and from pre-reconstructed structures can be generated. Moreover, as we will show below, our stochastic optimization procedure possesses excellent convergence behavior and is highly robust to noise in the projection data. We demonstrate the utility of our procedure by applying it to reconstruct a variety of

material microstructures in 2D and 3D and to quantitatively examine the information content of a given tomography data set. We find that highly accurate reconstructions can be obtained using only 20 to 40 projections for the systems that we consider here. This suggests that the typical tomography data set that includes thousands of projections for a single microstructure may contain redundant structural information that can be possibly reduced to a much smaller minimal set without losing the accuracy in reconstruction compared to those obtained from the larger data sets.

We explain our reconstruction procedure by considering a 2D binary material and the associated tomography data sets (i.e., projections) that are obtained using 2D parallel beam geometry. However, our procedure is general and can be applied to multiple phase materials, and other projection geometries. As schematically shown in Fig. 1, parallel rays are sent through a material and a detector behind the material can register the intensity of the rays passing through the sample. If we denote the position of a ray at the detector by r for the projection associated with angle θ, the total attenuation of the ray $p(r, \theta)$ due to absorption is given by

$$p(r,\theta) = \ln(J / J_0) = -\int \mu(x,y) ds \,, \tag{1}$$

where J_0 and J are the intensity of the incident and attenuated ray, respectively, and

$$\mu(x,y) = \mu_1 I^{(1)}(x,y) + \mu_2 I^{(2)}(x,y) \,, \tag{2}$$

and μ_i is the attenuation coefficient of phase i and $I^{(i)}$ is the indicator function of phase i, which is equal to 1 if the point is in phase i and equal to 0 otherwise, i.e.,

$$I^{(i)}(x,y) = \begin{cases} 1 & (x,y) \in V^{(i)} \\ 0 & otherwise \end{cases} . \tag{3}$$

It can be seen that the phase indicator functions completely specify the material microstructure [1]. Thus, the goal of tomography reconstruction is to recover the phase indictor functions $I^{(i)}$ from the total attenuation (i.e., the projections) at different angles $p(r, \theta)$.

Our reconstruction procedure is inspired by the stochastic optimization scheme developed by Yeong and Torquato to generate virtual microstructures from prescribed statistical morphological descriptors of the microstructure, i.e., various correlation functions associated with different phases of the material [30-33]. It works as follows. Given a prescribed set of tomographic projections (i.e., a set of

total attenuation values at prescribed angles $p(r, \theta)$ associated with a binary material), a trial binary microstructure is randomly generated (e.g., by assigning a phase to a pixel with certain probability). Then the attenuations values $p(r, \theta)$ associated with the trial microstructure at corresponding angles are computed. We define an energy functional E associated with the trial microstructure, which is the sum of the squared difference between the prescribed (p^*) and trial attenuation (p) values, i.e.,

$$E = \sum_{\theta} \sum_{r} \left[p(r,\theta) - p^*(r,\theta) \right]^2 \tag{4}$$

Thus, the reconstruction problem is formulated as an energy minimization problem in which the trivial microstructure evolves in order to lower the associated energy E. Ideally, the "ground-state" trial microstructure, i.e., the one with $E = 0$ possesses a set of total attenuations that is identical to the actual microstructure. Such a "ground-state" structure is considered the reconstruction of the actual microstructure.

The energy minimization problem is solved using a simulated annealing procedure [34]. Specifically, given an old (or initial) trial microstructure (with an energy E_{old}), a new trial microstructure is generated by changing a randomly selected pixel of phase i to phase j ($i \neq j$); or by switching the position of two randomly chosen pixels belonging to different phases. The former operation is to change the volume fraction of the phases while the latter is to re-distribute the phases to change the morphology of the trial microstructure. After a new trial microstructure is generated, its energy E_{new} is computed using Eq. (4). The probability that this new trial microstructure will be accepted and will replace the old trial microstructure in the course of the evolution is given by

$$p_{acc}(old \rightarrow new) = \min\left\{1, \quad \exp\left(\frac{E_{old}}{T}\right) \Big/ \exp\left(\frac{E_{new}}{T}\right)\right\} \tag{5}$$

where T is an effective temperature. In the beginning of the simulated annealing process, T is chosen to be high, leading to an acceptance probability of roughly one half. Then the temperature is gradually decreased according to a prescribed "cooling schedule". In this way, the system is allowed to explore a sufficiently large configuration space so that it will not get stuck in shallow local energy minima. In this work, we use an exponential cooling schedule, i.e., $T(t)/T_0 = \gamma^t$, where $0.95<\gamma<0.99$. We note that although discrete reconstruction approaches using simulated annealing [35] or level-set method [36] were applied to reconstruct geometrically simple objects (e.g., the cross-section of a blood vessel) from a small number of projections, to the best of our knowledge, no stochastic optimization scheme

has been devised for the reconstruction complex heterogeneous materials from limited tomography data.

To demonstrate the utility of our stochastic procedure, we have applied it to reconstruct a variety of material microstructures in 2D and 3D. For each target microstructure, we *compute* the associated set of projections (i.e., total attenuations) obtained by sending incident parallel rays at angles θ that are evenly distributed over [0, π], using Eq. (1). Without loss of generality, we have used $\mu_1 = 1$ and $\mu_2 = 0$ for the binary materials. The number of projections used in a reconstruction is denoted as N_θ. In the subsequent reconstruction examples, the final energy Eq. (4) (or the "error" between the target and reconstructed attentions at corresponding angles) is smaller than 10^{-5}.

Figure 2A shows a 2D binary model microstructure that mimics a eutectic layered structure. The simulated projections at $\theta = 0$ and π/2 in *parallel beam* geometry are shown in Fig. 2B. We use several different numbers of the projections for reconstructing this microstructure, i.e., N_θ = 5, 10, 20, and 40, in order to examine the information content of the tomographic data obtained at limited angles. The reconstructed microstructures are shown in Fig. 2C. An initial increase of the number of projections N_θ (e.g., from 5 to 10 and from 10 to 20) can lead to significantly improved reconstructed microstructures. However, further increasing N_θ (e.g., from 20 to 40) does not result in much improvement of the accuracy. To quantify the accuracy of the reconstructions, we introduce the following metric:

$$M_a = \sum_{x,y} \left| I(x,y) - I^*(x,y) \right| / N^2 \qquad (6)$$

where $I(x,y)$ is the indicator function of the colored phase in the reconstructed microstructure and $I^*(x,y)$ is the indicator function of the black phase in the target microstructure. In other words, M_a is simply the fraction of misplaced pixels over the total number of pixels in the system. Figure 2D shows M_a as a function of N_θ for the model microstructures we studied. One can see quantitatively that as N_θ increases, M_a initial decreases and then reaches a plateau, i.e., further increasing the number of projections does not significantly improve accuracy any more. This is consistent with the visual comparisons of the reconstructed and target microstructures.

Figure 3 shows the reconstruction of a model microstructure composed of equal-sized spheres in a matrix (generated via Monte-Carlo simulations) (upper panels) and the reconstruction of a lead-tin alloy [37] in 3D (lower panels). In particular, 30 parallel/cone beam projections are used for the sphere-packing/alloy microstructure (see Figs. 3A and D). Again, it can be seen that the reconstructions (Figs. 3C and F) are virtually identical to the corresponding actual structures (Figs. 3B and E). The associated accuracy metrics M_a are respectively 0.048 and 0.035 for the sphere-packing and the lead-tin alloy structures.

Finally, we show that our reconstruction procedure is sufficiently robust to noises in the projection data. We introduce noises in the simulated projection data by randomly varying the totally attenuation values in each detector bin with a prescribed average amount and use the perturbed data as input for the reconstruction algorithm. Figure 4A shows the target image (i.e., a model microstructure of particle reinforced composite) and B, C and D show the reconstructions from noisy projection data randomly perturbed by 1%, 5% and 10%. As the noise level increases, more and more matrix-associated (black) pixels are found in the particle phase, which decreases the quality of reconstruction. However, the shape, size and spatial distributions of the particle phase are still apparent even at the highest noise level. These results clear indicate the robustness of our stochastic reconstruction method against noise. Stochastic reconstructions from experimental tomography data to be reported elsewhere [38] also suggest that our procedure is sufficiently robust to noises from different sources.

In summary, we have presented here a stochastic procedure to accurately reconstruct material microstructures from limited-angle projections. We have demonstrated the utility of this procedure by applying it to successfully reconstruct a number of complex microstructures. Our procedure also allowed us to elucidate the information content of the limited tomography data by quantitatively comparing the reconstructed microstructures to the target material. The fact that only a relative small number of projections are sufficient for each static microstructure suggests that our procedure could have fruitful applications in characterizing microstructure evolution over time (i.e., 4D materials science). For example, one could significantly improve the temporal resolution for the characterization of fast processes such as instable crack growth.

This work was supported by the Division of Materials Research at the National Science Foundation under award No. DMR-1305119 (Dr. Diana Farkas, program manager). Y. J. also thanks Arizona State University for the generous start-up funds.

References

[1] Torquato S. Random Heterogeneous Materials: Microstructure and Macroscopic Properties. New York: Springer; 2002.

[2] Sahimi M. Heterogeneous Materials I: Linear Transport and Optical Properties. New York: Springer; 2003.

[3] Thornton K, Poulsen HF. MRS Bull 2008; 33: 587.

[4] Brandon D, Kaplan WD. Microstructural Characterization of Materials, 2nd Ed. Wiley; 2008.

[5] Baruchel J, Bleuet P, Bravin A, Coan P, Lima E, Madsen A, Ludwig W, Pernot P, Susini J. C R Physique 2008; 9: 624.

[6] Kinney JH, Nichols MC. Annu Rev Mater Sci 1992; 22: 121.

[7] Kak A, Slaney M. Principles of Computerized Tomographic Imaging. IEEE Press; 1988.

[8] Feldkamp LA, Davis LC, Kress JW. J Opt Soc Am 1984; A6: 612.

[9] Kupsch A, Lange A., Hentschel MP. Enhanced spatial resolution in 2D CT-reconstruction without filtered back projection: DIRECTT, WCNDT Shanghai, 2008.

[10] Babout L, Maire E, Buffière JY, Fougères R. Acta Mater 2001; 49: 2055.

[11] Borbély A, Csikor FF, Zabler S, Cloetens P, Biermann H. Mater Sci Eng A 2004; 367: 40.

[12] Kenesei P, Biermann H, Borbély A. Scr Mater 2005; 53: 787.

[13] Weck A, Wilkinson DS, Maire E, Toda H. Acta Mater 2008; 56: 2919.

[14] Toda H, Yamamoto S, Kobayashi M, Uesugi K, Zhang H. Acta Mater 2008; 56: 6027.

[15] Williams JJ, Flom Z, Amell AA, Chawla N, Xiao X, De Carlo F. Acta Mater 2010; 58: 6194.

[16] Williams JJ, Yazzie KE, Phillips NC, Chawla N, Xiao X, De Carlo F, Iyyer N, Kittur M. Metall Mater Trans 2011; 42: 3845.

[17] Herman, G. T. and Kuba, A., Discrete Tomography: Foundations, Algorithms, and Applications, Birkhäuser Boston, 1999.

[18] Herman, G. T. and Kuba, A., Advances in Discrete Tomography and Its Applications, Birkhäuser Boston, 2007.

[19] R.J. Gardner, P. Gritzmann, Trans. Amer. Math. Soc. 349 (1997), 2271-2295.

[20] L. Hajdu, R. Tijdeman, J. Reine Angew. Math. 534 (2001), 119-128.

[21] S. Brunetti, A. Del Lungo, P. Gritzmann, S. de Vries, Theoret. Comput. Sci. 406 (2008), 63-71.

[22] P. Gritzmann, B. Langfeld, European J. Combin. 29 (2008), 1894-1909.

[23] H.J. Ryser, Matrices of zeros and ones, Bull. Amer. Math. Soc. 66 (1960) 442-464.

[24] E. Barcucci, S. Brunetti, A. Del Lungo, M. Nivat, Discrete Mathematics 241 (2001), 65-78.

[25] Batenburg, Joost; Sijbers, Jan, IEEE Tran. Image Proc. 20 (2011) 2542-2553.

[26] W. van Aarle, K J. Batenburg, and J. Sijbers, IEEE Tran. Image Proc. 21 (2012) 4608.

[27] K. J. Batenburg, and J. Sijbers, Discrete Applied Mathematics 157 (2009) 438-451.

[28] A. Alpers, H.F. Poulsen, E. Knudsen, G.T. Herman, Journal of Applied Crystallography 39 (2006) 582-588.

[29] L. Rodek, H.F. Poulsen, E. Knudsen, G.T. Herman, Journal of Applied Crystallography 40 (2007) 313-321.

[30] Yeong CLY, Torquato S. Phys Rev E 1998; 57: 495.

[31] Jiao Y, Stillinger FH, Torquato S. Phys Rev E 2008; 77: 031135.

[32] Gommes CJ, Jiao Y, Torquato S. Phys Rev Lett 2012; 108: 080601.

[33] Gommes CJ, Jiao Y, Torquato S. Phys Rev E. 2012; 85: 051140.

[34] Kirkpatrick S, Gelatt CD, Vecchi MP. Science 1983; 220: 671.

[35] Robert N, Peyrin F, Yaffe MJ. Med Phys 1994; 21: 1839.

[36] Alvino CV, Yezzi AJ Jr. Tomographic reconstruction of piecewise-smooth images. Proceedings of the 2004 IEEE Computer Conference (CVPR'04).

[37] Jiao Y, Padilla E, Chawla N. Acta Materialia 2013; 61: 3370.

[38] Li H, S. Kaira, Mertens J, Williams JJ, Chawla N, Jiao Y, in preparation.

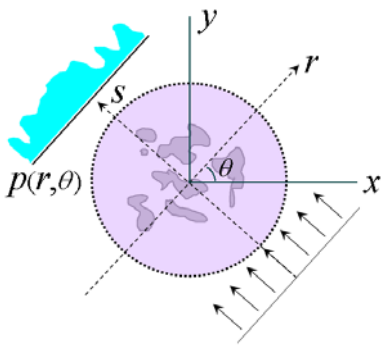

Fig. 1: A schematic illustration of a parallel-beam tomography system. The incident rays are parallel to one another and are attenuated as they pass through the material sample. The intensity of the attenuated rays is obtained using a detector, from which the total attenuation $p(r, \theta)$ can be computed. This figure schematically shows a profile of the total attenuation associated with angle θ.

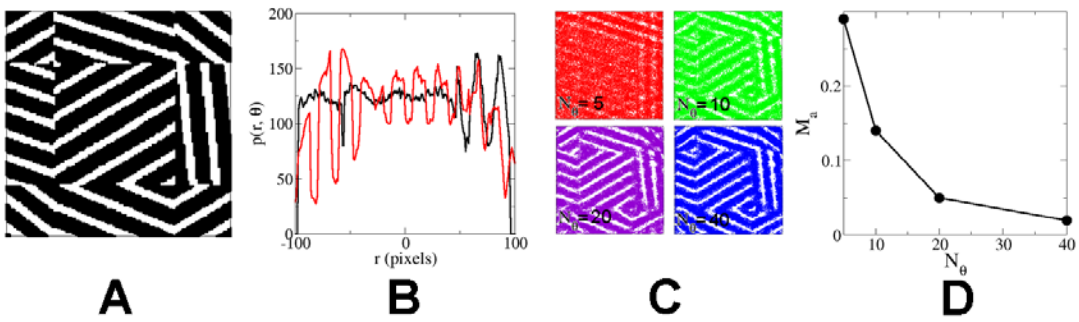

Fig. 2: Target 2D model microstructure that mimics typical eutectic structures (A) and the associated simulated parallel beam projections (B) at angles 0 (black curve) and π/2 (red curve). (C) Reconstructed microstructures from limited-angle projections via the stochastic procedure. The number of projections N_θ used for the reconstructions are given in the plot. It can be seen that as increases N_θ, the accuracy of the reconstructions is improved. (D) The accuracy metric M_a as a function of N_θ, which rapidly decays initially as N_θ increases.

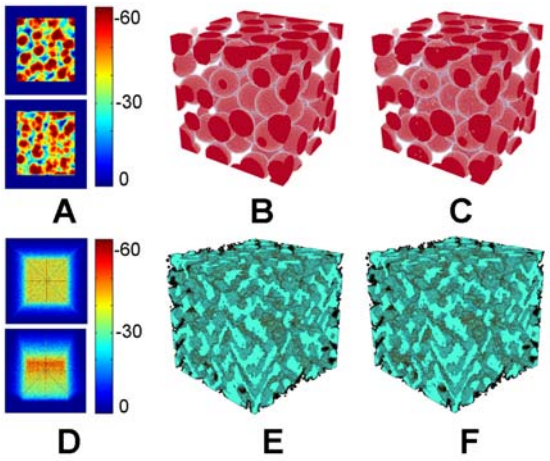

Fig 3: Upper panels: The reconstruction of a packing of equal-sized spheres in a matrix. The linear size of the system is 100 μm. (A) The simulated projections at $\theta = 0$ (upper panel) and π/2 (lower panel) associated with the structure. The colors indicate the rescaled total attenuation of the incident ray along a particular path, which is effective the total distance the ray travels within a material phase. The unit of the rescaled total attenuation is the length a pixel. (B) The target microstructure. (C) The reconstructed microstructure. Lower panels: The reconstruction of a lead-tin binary alloy. The linear size of the system is 60 μm. (D) The simulated projections at $\theta = 0$ (upper panel) and π/2 (lower panel). (E) The target microstructure. (F) The reconstructed microstructure.

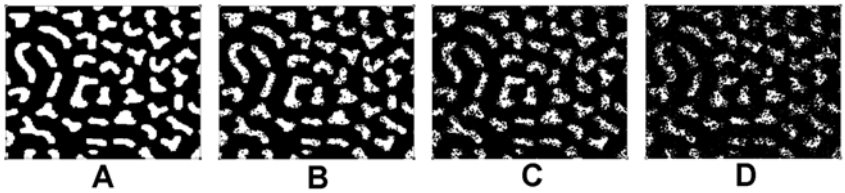

Fig. 4: Reconstruction of a model microstructure of a particle-reinforced composite material (A) from projection data with 1% (B), 5% (C) and 10% noise (D).